International Journal of Multiphase Flow 36 (2010) 375–384

Contents lists available at ScienceDirect

International Journal of Multiphase Flow

journal homepage: www.elsevier.com/locate/ijmulflow

Experimental study of critical heat flux enhancement during forced convective flow boiling of nanofluid on a short heated surface

Ho Seon Ahn [a], Hyungdae Kim [b], HangJin Jo [a], SoonHo Kang [a], WonPyo Chang [c], Moo Hwan Kim [a,*]

[a] Department of Mechanical Engineering, POSTECH, Pohang 790-784, Republic of Korea
[b] Department of Nuclear Science and Engineering, Massachusetts Institute of Technology, USA
[c] Korea Atomic Energy Research Institute, Republic of Korea

ARTICLE INFO

Article history:
Received 3 May 2009
Received in revised form 31 December 2009
Accepted 11 January 2010
Available online 14 January 2010

Keywords:
Forced convective boiling
Critical heat flux
Nanofluid

ABSTRACT

Enhancements of nucleate boiling critical heat flux (CHF) using nanofluids in a pool boiling are well-known. Considering importance of flow boiling heat transfer in various practical applications, an experimental study on CHF enhancements of nanofluids under convective flow conditions was performed. A rectangular flow channel with 10-mm width and 5-mm height was used. A 10 mm-diameter disk-type copper surface, heated by conduction heat transfer, was placed at the bottom surface of the flow channel as a test heater. Aqueous nanofluids with alumina nanoparticles at the concentration of 0.01% by volume were investigated. The experimental results showed that the nanofluid flow boiling CHF was distinctly enhanced under the forced convective flow conditions compared to that in pure water. Subsequent to the boiling experiments, the heater surfaces were examined with scanning electron microscope and by measuring contact angle. The surface characterization results suggested that the flow boiling CHF enhancement in nanofluids is mostly caused by the nanoparticles deposition of the heater surface during vigorous boiling of nanofluids and the subsequent wettability enhancements.

1. Introduction

Nanofluids are engineered heat transfer fluids consisting of nano-sized particles (nanoparticles) dispersed in a base liquid. These fluids have been studied in various fields of thermal engineering since Choi (1995) showed abnormally improved thermal properties of nanofluids. You et al. (2003) found that adding tiny amounts (less than 0.001% by volume) of alumina nanoparticles to a conventional cooling liquid could significantly increase the critical heat flux (CHF) up to ~200%. However, such a large CHF enhancement in nanofluids could not be interpreted using traditional CHF theories, such as hydrodynamic instability models (Kutateladze, 1950; Zuber, 1959). Because of its potential for remarkable CHF enhancement and scientific interest about its mechanism, boiling heat transfer research of nanofluids has attracted considerable attention, especially from those concerned with CHF.

Vassallo et al. (2004) reported that aqueous suspensions of 0.5 vol.% 15.5 nm and 3 μm SiO_2 particles increased the CHF up to 60%, and did not affect to nucleate boiling heat transfer. Park et al. (2004) studied that the film boiling heat transfer in Al_2O_3–water nanofluid as well as pure water through the quenching test, and reported that the nanoparticle deposition on the sphere surface prevented the formation of the a stable vapor film. Moreno et al. (2005) observed no change in boiling heat transfer coefficient but a significant improvement in CHF (up to ~200%) in Al_2O_3–water, ZnO–water and Al_2O_3–ethylene glycol nanofluid. Milanova and Kumar (2005) reported that the CHF increased more, as the higher pH levels (up to 12.3) of SiO_2 nanoparticles–water nanofluids, relatively little influence on the nucleate boiling regime. Wen and Ding (2005) observed up to 40% enhancement in nucleate boiling. They only interpreted the attribution of the stability of nanofluids about this enhancement, which did not deposit on the surface. Separately, Bang and Chang (2005) reported that the CHF in Al_2O_3–water nanofluids is enhanced by up to 51% compared to pure water but the boiling heat transfer coefficient is considerably degraded. They hypothesized that the plausible reason for the changes in boiling heat transfer performance was the nanoparticle deposition onto the surface, which was confirmed by the surface roughness measurement after nanofluid boiling tests and the consequent change in nucleate site density. Kim et al. (2006a,b) carried out pool boiling CHF experiments of pure water on a nanoparticle-fouled heater as a result of a pre-boiling in nanofluid, and showed an interesting result that the same magnitude of the significant CHF increase in nanofluid was observed for the nanoparticle-fouled surface submerged even in pure water. This suggested that the CHF increase in nanofluids is caused by the altered surface

* Corresponding author. Tel.: +82 54 279 2165; fax: +82 54 279 3199.
E-mail address: mhkim@postech.ac.kr (M.H. Kim).

0301-9322/$ - see front matter © 2010 Elsevier Ltd. All rights reserved.
doi:10.1016/j.ijmultiphaseflow.2010.01.004

characteristics due to the surface deposition of nanoparticles during the nanofluid boiling. The same results were recently obtained by Golubovic et al. (2008). Therefore, it was suggested that the improvements of interfacial parameters due to nanoparticles fouling might be key factors in the significant increase in CHF of nanofluids. Therefore, investigations into the mechanism of the critical heat flux increase in the boiling of nanofluids should seek effects of both the nanoparticles in the fluid (nanofluids) and the nanoparticles deposited on the surface (Liter and Kaviany, 2001).

The deposition of the nanoparticles on the boiling surface changes the microstructure and the physicochemical properties. Such changes in the heat transfer surface exert strong influences on the boiling phenomena by changing key parameters such as nucleation site density, bubble departure diameter and frequency, and evaporation of the micro and macrolayer beneath the growing bubbles. On the other hand, Kim et al. (2007a) reported that the nanoparticle-fouled surfaces had significantly increased wettability, as measured by a reduction in the static contact angle. They based their suggestion on a review of the prevalent CHF theories, stating that the improved wettability caused by the nanoparticle layer could predict CHF enhancement. Liu and Liao (2008) and Coursey and Kim (2008) performed pool boiling experiments with water-based and alcohol-based nanofluids on a plain heated surface. Both studies confirmed it from static contact angle measurements that the nanoparticle layer formed on the heater surface significantly improved wettability. Coursey and Kim (2008) also showed that surface treatments such as oxidation alone resulted in CHF enhancement similar to nanofluids. Thus, the previous studies suggest that the likely CHF enhancement mechanism for nanofluids is an improvement in the ability of the fluid to wet the surface because of a thin nanoparticle sorption layer formed by evaporation of the microlayer containing nanoparticles underneath a bubble growing at the heated surface (Kim and Kim, 2007).

Recently, convective flow boiling of nanofluids was studied by Kim et al. (2008, 2009a) in the circular stainless steel tube using the electrical heating. They reported significant increases in flow boiling CHF of nanofluids with alumina, diamond, and zinc oxide that the contact angle on the tube decreased to control the concentration of nanofluid. Also, they found in the higher concentration of nanofluid, the CHF enhancement was higher and the static contact angle on the fouled surface was lower. It was concluded from their experiments that the improved surface wettability due to the nanoparticles deposition layer caused the significant CHF enhancements during the convective flow boiling of nanofluids, which is consistent with findings of the previous pool boiling research. However, their results could be questioned about electrical heating in nanofluid. Many previous nanofluid studies (e.g., Kim et al., 2006a,b; Kim, 2007; Kim and Kim, 2007a,b; Golubovic et al., 2008; Kim et al., 2008, 2009a,b) have also carried out the pool boiling experiments on electrically heated metallic wires or surfaces. Applying an electric potential to heat the thin wire or the metallic tube can cause nanoparticles in the liquid to migrate and accumulate on the heater surface, which is well-known as the electrophoretic phenomenon in electrolytes (Santillan et al., 2008). Thus, the technique of direct electric heating of the boiling surface could contribute to the nanoparticle deposition, distorting the boiling characteristics of nanofluids. Therefore, for our flow boiling experiments we decided to heat the boiling surface using conduction heat transfer from a high temperature object. In addition, we decided to fix the concentration of nanofluid as 0.01 vol.% for investigating the relation between CHF enhancement and a given flow velocity in this study. And our test specimen was a flat and short surface to measure the change of surface characteristics easily furthermore, i.e. the static contact angle and SEM image. The CHF enhancement ratio ($CHF_{nanofluid}/CHF_{purewater}$) at a given flow velocity would be analyzed by the Kandlikar's pool boiling model. Additionally, we purposed the consistence of CHF enhancement in nanofluid to verify the surface effect through the pure water boiling test using nanoparticles coated specimen. Through the investigation of surface, before and after of the coated specimen, the effect of flow momentum on the nanoparticles-coated surface would be presented.

2. Experiments

2.1. Preparation and characterization of nanofluids

In this study, nanofluids were prepared by two-step method that dry nanoparticles disperse into a base fluid. Dry nano-sized alumina particles (Al_2O_3) were dispersed in distilled water (pure water) without any additive. For a single experimental test, about seventy liter nanofluid was prepared in a boiling pool, which has an ultrasonic vibrator to directly disperse the dry nanoparticles into base liquid. In this study, 0.01 vol.% nanoparticle concentration was used because the previous research shows that the dilute nanofluids of 0.01 vol.% were enough to cause an extraordinary CHF enhancement in the pool boiling condition (Kim et al., 2007b). Fig. 1 shows the nanoparticles dispersed in the prepared nanofluid. The Al_2O_3 nanoparticles were spheres with a mean diameter of 47 nm and a range from 10 to 100 nm, as estimated from TEM images.

The amount of nanoparticles dispersed in the solution was quantified by volume concentration and not by mass concentration because it is known that the flow phenomenon of a liquid–solid suspension depends on the hydrodynamic force acting on the surface of the solid particles. However, because it is very difficult to directly measure the precise true volume of nanoparticles, the following conversion formula is conventionally used to calculate the volume concentration (ϕ_V) of nanoparticles in nanofluid (Bang and Chang, 2005).

$$\phi_V = \frac{1}{\left(\frac{1-\phi_m}{\phi_m}\right)\frac{\rho_p}{\rho_f} + 1} \tag{1}$$

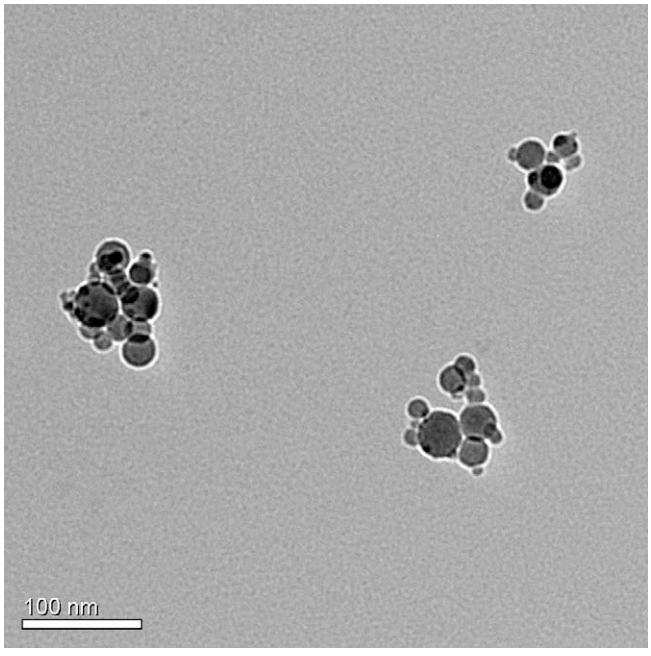

Fig. 1. Transmission electron microscopy (TEM) picture of alumina nanoparticles dispersed in pure water.

where ϕ_m is the mass concentration of nanoparticles, ρ_p is the nanoparticle density, and ρ_f is the liquid density. Thermal conductivity enhancement is a very important physical property of a nanofluid as a cooling fluid. However, the volume concentrations in the present work were too low to expect a considerable enhancement of thermal conductivity (Murshed et al., 2005). For the same reason, the viscosity and density also had nominal changes (Kim et al., 2009a,b).

2.2. Convective flow boiling

2.2.1. Forced convective flow boiling facility

Various recent studies on nanofluid have reported that CHF enhancements in nanofluids under pool boiling conditions mainly were resulted from the deposition of nanoparticles on the surface. With this perspective, the present experimental apparatus was designed to enable investigation of the heating surface under the flow boiling condition. Therefore, an external flow boiling system rather than a circular tube boiling system was chosen to allow surface investigation. Fig. 2 shows the schematic diagram of the experimental apparatus, which includes nanofluid, a magnetic pump, a circulation loop, and a pool for convective flow. The pool has a test section and a rectangular channel that induces flow to the test section.

The main pool consists of a boiling chamber that contains de-ionized distilled water or nanofluid, a heating system, a test section, an ultrasonic vibrator, and a rectangular channel. The boiling chamber has a size of 1520 mm (length) × 120 mm (width) with a height of 540 mm and is made of an aluminum alloy. There are three cartridge heaters of the immersion type with a peak heating power of 9000 W. Four T-type thermocouples are immersed in the pool to measure the temperature of the bulk fluid. During the experiment, the bulk temperature was maintained at 100 °C by feedback control between the thermocouples and the pool heaters. Four reflux condensers are located at the top of the chamber to condense vapor. Four rectangular polycarbonate windows are on the front and back walls to visualize flow in the channel as well as boiling phenomenon inside the chamber. The ultrasonic vibrator was used to disperse the nanoparticles in the water with a peak vibrating frequency of 40 kHz and power of 1200 W. Twenty-four vibrators are located on the top of the pool. A rectangular channel made of transparent strengthened acryl with a cross section of 10 mm (width) × 5 mm (height) and a length of 1.2 m was set up on the bottom of the pool chamber. Working fluids (de-ionized distilled water or nanofluids) leaving the pool chamber with a saturated state circulated through the loop and entered the pool chamber again. At this time, the circulated working fluid was driven into the rectangular channel and entered the test section. The length of the channel was designed to maintain a fully developed flow by considering both the entrance length and the maximum Re. A HP Agilent 34970A data acquisition system and a personal computer were used to collect and analyze all data from the temperature sensors.

The loop section consisted of a magnetic pump to circulate working fluids, two flow meters, a heat exchanger to drop the temperature of working fluids below 100 °C, a circulation heater to raise the temperature of working fluid to 100 °C, and a PID feedback controller. The entire loop was constructed of 3/4 in. SUS316 tube. The total pressure drop of the tube for single phase flow was ignored because it was estimated to be a very small value of approximately 47 Pa. The flow rate of the magnetic pump was controlled through DC voltage control. This pump has a maximum flow rate capacity of 26 l/min and a maximum operating temperature of 130 °C. The heat exchanger was a regular OMEGA product of the shell and multi-tube type. There are two K-type thermocouples at the inlet and the outlet of the heat exchanger. The inlet temperature was fixed at 99.5 °C. The outlet temperature could be controlled by the flow rate of tap water. The tap-water flow rate was set to avoid the cavitation in the pump and varied depending on the flow velocity in the channel of the pool chamber. During the experiment, the flow temperature was maintained around 99.5 °C by feedback control between the K-type thermocouple at the outlet of the pre-heater and the pre-heater made by OMEGA. The two flow meters (OMEGA) could adjust the flow rate in two control ranges, i.e., flows of 0.35–3.5 GPM and 4–60 GPM or velocities of 0.2–2.2 m/s and 2.5–37.9 m/s. Pictures of all components of this experimental apparatus are included in a previous research report (Ahn et al., 2008a).

2.2.2. Test heater and data acquisition

Fig. 3 shows the schematics of the test heater used in the present work. The test heater is a 10 mm-diameter cylindrical copper block whose side wall is insulated by PEEK. Heat is transferred through the high graded cylindrical copper block to the test heater

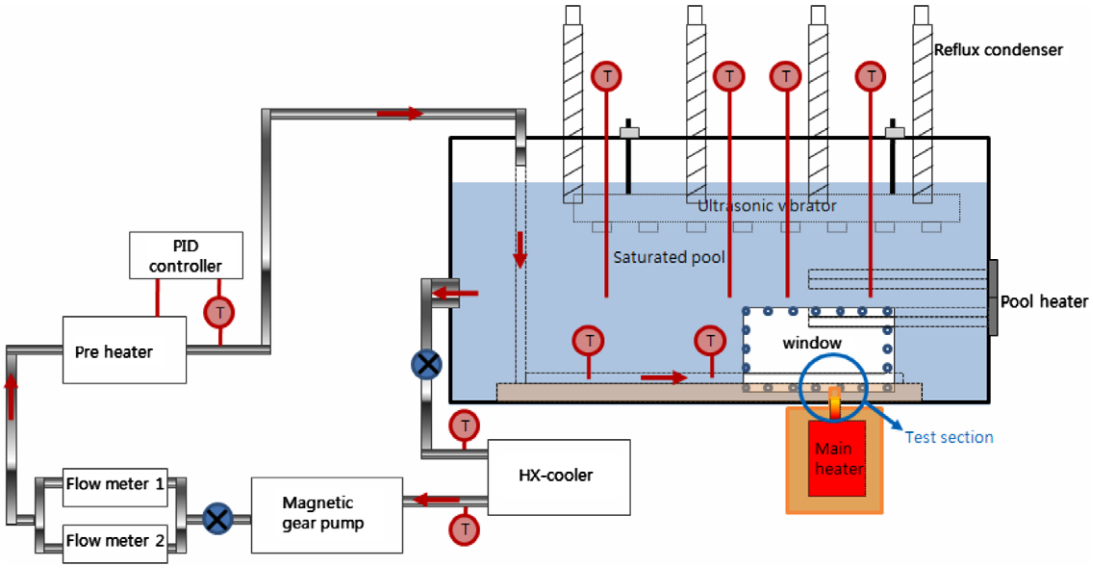

Fig. 2. Schematic of a flow boiling CHF experimental facility.

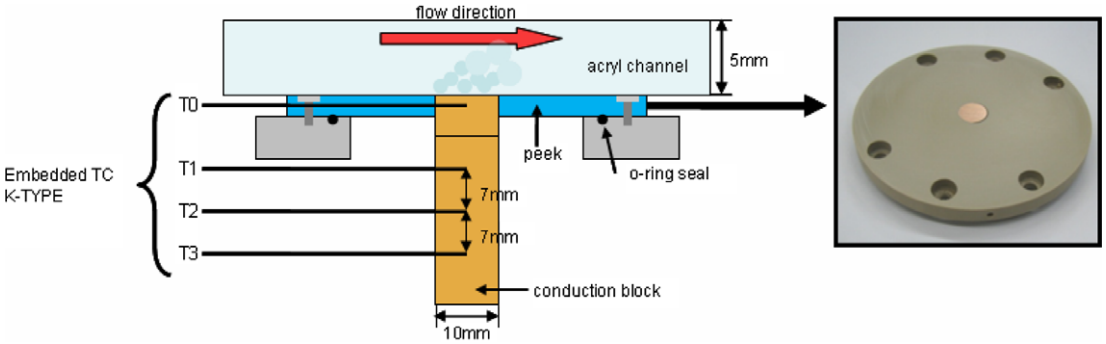

Fig. 3. Schematic of a conductive test heater.

by means of thermal conduction, and it leaded to boiling of cooling liquid on the top surface of the specimen. The test heater was detachable for the investigating of the surface at the end of the experiment. The test section was drilled through the PEEK insulator from the side to install a 0.5 mm OD K-type thermocouple at the center. Before and after each boiling test, the heater surface was characterized in five different points using a three-dimensional profiler (VEECO, optical surface profiler) (Fig. 4).

The heating system consists of 10 cartridge heaters with a peak heating power of 500 W per heater, a conductive copper block for transfer and concentration of the heat generated from the cartridge heaters, and a high grade (99.999%) cylindrical copper block that measures the heat flux and transfers the heat to the test section. The copper block is insulated by a high temperature insulating material with a very small thermal conductivity of 0.1 W/m/K. Consequently, heat transfer through the cylindrical copper block could be simplified to a one-dimensional conduction heat transfer problem. Three K-type thermocouples are embedded in the cylindrical copper block along the center at 7 mm intervals. The heat flux was calculated using the one-dimensional, steady-state conduction heat transfer equation as follows.

$$Q'' = k \times \frac{\Delta T}{\Delta x} = k \times \frac{T_2 - T_1}{\Delta x} \tag{2}$$

where T_1 and T_2 are the temperatures recorded in the conductive copper block, q'' is the measured heat flux (kW/m^2), k is the thermal conductivity (W/m K) and Δx is the distance between temperature measurement points in the conduction copper block (m). Note that the linear relationship among the three temperature measurements in the cylindrical copper block was examined with a numerical simulation for the steady-state heat conduction in the actual heater geometry using the commercial software, FLUENT 6.0 (Ahn et al., 2008b), and the numerical simulation results confirmed that, Eq. (2) is proper to estimate the heat flux. Then the wall superheat (Eq. (3)) was calculated by extrapolating the temperature T_0 measured inside the test heater, using the heat flux obtained in Eq. (2):

$$\Delta T_{wall} = T_{wall} - T_{sat} = \left(T_0 - \frac{\dot{q}''}{k} d\right) - T_{sat} \tag{3}$$

where ΔT_{wall} is the wall superheat and T_{wall} is the surface wall temperature, T_{sat} is the saturated temperature of bulk fluid and d is the distance between the T_0 measured point and the surface.

2.2.3. Procedure of experiment

After the test section was set up, working fluids (de-ionized distilled water or nanofluid) were pushed into the pool chamber with the installed magnetic pump. The flow direction could be changed by a valve selection. For an experiment with nanofluid, nanoparticles were dispersed for 3 h to prepare the nanofluid, and it was then heated up to saturation temperature. A degassing process was performed once during the heating up to the bulk temperature of 100 °C. After the degassing process, the pump, heat exchanger, and circulation heater were operated until they reached steady-state. The steady-state was the condition in which the bulk temperature was the same as the outlet temperature of the circulation heater at 99.5 °C. When the condition of the experiment reached steady-state, the main heater was switched into the power control mode. As previously described, the response time of the main heater was very slow because heat transfer occurred by conduction through a massive copper block. The heating process in the specimen could be defined as a quasi-steady-state. As soon as CHF occurred, the heat flux estimated from the temperature gradient dropped rapidly with a sudden increase in wall temperature. After CHF observation, a z-directional level meter of the main heater was controlled to break the contact between the specimen and the cylindrical copper block. This method was necessary to protect the PEEK insulator around the specimen from melting. The flow velocity at the test section in the channel was measured by the flow meter. Water flow passed through a heating zone inside the channel. The heating zone was a heater specimen to which heat was transferred through the cylindrical copper block.

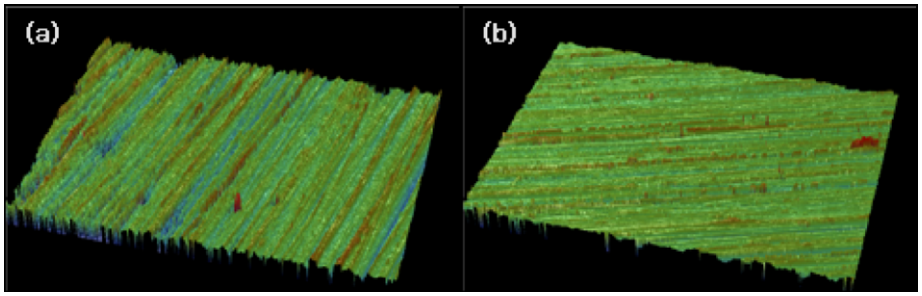

Fig. 4. Surface profiler measurement: (a) as-received specimen; (b) a water-boiled specimen.

2.2.4. Uncertainty analysis

The wall temperature and heat flux were measured using K-type thermocouples. The thermocouples were calibrated using a reference RTD temperature sensor with the maximum measurement error of ±0.1 K, and thus it could be assumed that the measurement error of the thermocouples were ±0.1 K. The surface heat flux was calculated by Eq. (2). The flow meters were calibrated using the balance, thus it could be assumed that the measurement error of the flow velocity were 2% at 1 m/s and 0.1% at 4 m/s. For the uncertainty of the heat flux, we applied the following equations (Coleman and Steele, 1999):

$$\frac{U_{q''}}{q''} = \sqrt{\left(\frac{U_{T_2-T_1}}{T_2-T_1}\right)^2 + \left(\frac{U_{\Delta x}}{\Delta x}\right)^2} \tag{4}$$

$$\frac{U_{\Delta T_{wall}}}{\Delta T_{wall}} = \sqrt{\left(\frac{U_{T_0-T_{sat}}}{T_0-T_{sat}}\right)^2 + \left(\frac{U_{q''}}{q''}\right)^2 + \left(\frac{U_d}{d}\right)^2} \tag{5}$$

where the parameters $U_{q''}$, U_{T2-T1}, and $U\Delta_x$ are the uncertainties of the heat flux q'', $T_2 - T_1$, and Δx, respectively. All the thermocouples were calibrated using a reference resistance temperature detector sensor with a measurement accuracy of ±0.2 K certificated by the Korea Testing Laboratory. Table 1 shows the uncertainty analysis results for the experimental conditions. The maximum uncertainties in the heat flux measurement were 0.75% at 2000 kW/m^2 and 10.2% at 100 kW/m^2.

3. Experimental result and discussion

3.1. Flow boiling CHF

Fig. 5 shows three boiling curves of pure water at a flow velocity of 3 m/s, which were conducted to validate reproducibility of the experimental facility. Onset of nucleate boiling occurs consistently at about 23 °C in all cases. Also boiling heat transfer characteristics including CHF were almost identical among tests. An average of three CHF values in pure water was about 2800 kW/m^2. Fig. 6 shows the CHF experimental data for de-ionized water at various flow velocities. Our water data were quite reproducible at each flow velocity, within ±3%. The results make a clear trend that the flow boiling CHF value increases as the flow velocity increases. Katto and Kurata (1980) investigated the external flow boiling CHF on a uniformly-heated, short plate heater in a parallel flow, which are similar conditions as the present study, and suggested an experimental correlation for pure water in the range of liquid velocity from 1.5 m/s to 10 m/s.

$$\frac{q''_{chf}}{GH_{fg}} = 0.186\left(\frac{\rho_v}{\rho_l}\right)^{0.559}\left(\frac{\sigma\rho_l}{G^2 l}\right)^{0.264} \tag{6}$$

where G is the mass flux (kg/s m^2), ρ the density (kg/m^3) of liquid (l) and vapor (v), σ the surface tension of bulk fluid (N/m), and l is the heating length (m). In fact, our experimental data shows a good agreement with Eq. (6) as shown in Fig. 6, suggesting that our follow boiling facility worked properly. Fig. 7 shows flow boiling curves for 3 m/s in pure water and nanofluid. The results for nanofluids shows a considerable scatter in boiling curve and CHF compared to those of pure water, however it is obvious that the nanofluid has the significantly higher flow boiling CHF. The measured flow boiling CHF results of pure water and alumina nanofluids for the velocity range from 0 m/s to 4 m/s are shown in Fig. 8. The

Table 1
Experimental uncertainties.

Variables	Uncertainty
Temperature (°C)	±0.1–0.2
Heat flux (kW/m^2)	±0.75–10.2%
Channel size (mm)	±0.2 (2%)
Flow velocity (m/s)	±0.1–2%

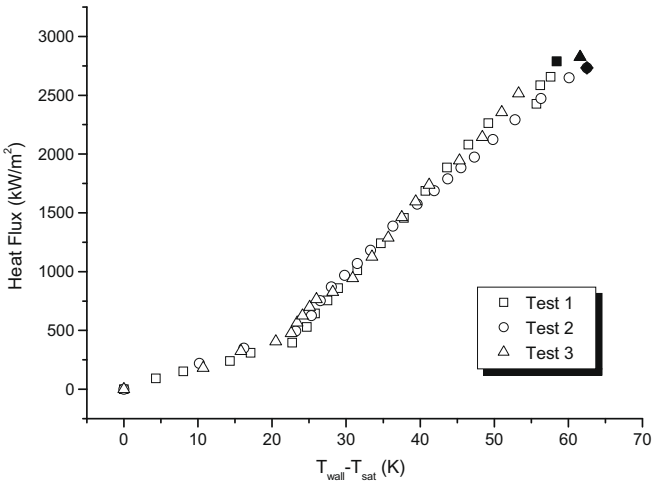

Fig. 5. Flow boiling curves of pure water 3 m/s in pure water.

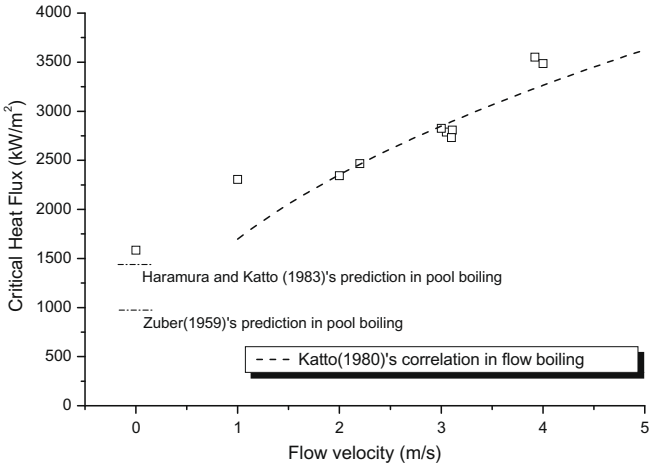

Fig. 6. Critical heat flux vs. flow velocity of pure water.

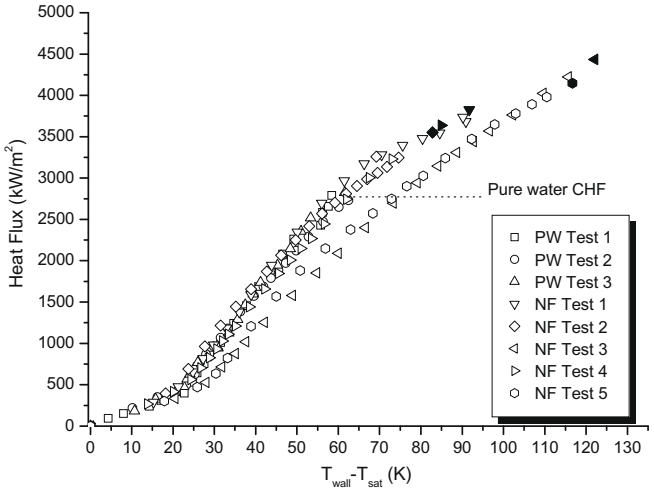

Fig. 7. Flow boiling curves for pure water and nanofluid 3 m/.

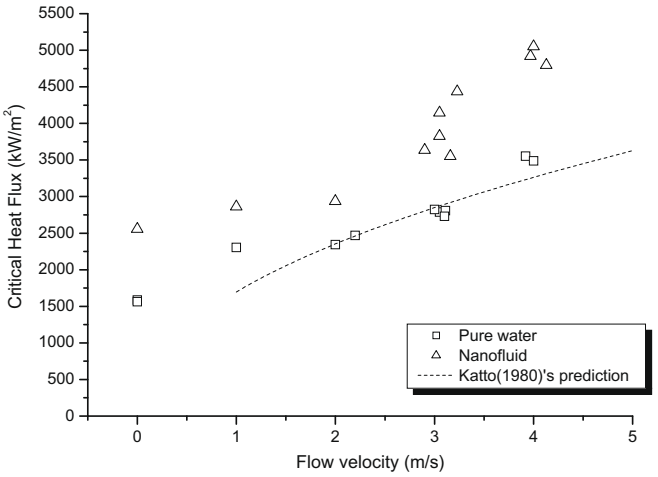

Fig. 8. Critical heat flux vs. flow velocity in pure water and nanofluid.

Table 2
Average CHF enhancement ratio as increasing the flow velocity.

Flow velocity(m/s)	CHF in pure water (kW/m^2)	CHF in nanofluid (kW/m^2)	Enhancement ratio (%)
0	1486	2242	51
1	2306	2864	24
2	2344	2938	25
3	2828	4012	42
4	3520	4923	40

nanofluids CHF data exist well above the water data for all flow velocities. The CHF enhancements in nanofluids compared to water CHF data at each velocity condition are summarized in Table 2. The enhancement for no flow condition at 0 m/s is about 50%, which is consistent with the pool boiling CHF experimental results obtained in the previous researched (Bang and Chang, 2005; Kim et al., 2010). Under the forced flow condition, the data for the low flow velocities ($\leqslant$2 m/s) show the relatively smaller CHF increases of ~25% compared to the 50% enhancement for no flow condition, and, the increase of the flow velocity above 2 m/s, however, causes a re-raise in the CHF enhancement up to ~42%. Accordingly, the present experimental results for various flow velocities show that nanofluids as a working fluid cause the significant CHF enhancements under the flow condition as well as under the pool condition.

3.2. Deposition of nanoparticles on the heating surface

Many recent studies for pool boiling of nanofluids (see e.g. Kim et al., 2006a, 2007b; Bang and Chang, 2005; Kim and Kim, 2007) reported that the key parameters of CHF enhancement in nanofluid were likely due to nanoparticles deposition during nucleate boiling of nanofluids and consequent changes of surface properties, such as morphology, wettability, and capillarity. Indeed, while the as-received and water-boiled surfaces are clean, the considerable nanoparticles deposition was observed on the heater surface subsequent to the flow boiling CHF experiments in nanofluid, as shown in Fig. 13. The well-known surface factors influencing CHF phenomena are substrate effusivity, surface roughness, and wettability (Arik and Bar, 2003; Chowdhury and Winterton, 1985).

Table 3
Thermo-physical properties of the heater materials and surface properties.

	Effusivity, $(\rho ck)^{1/2}$ (J/(m K s$^{1/2}$))	Density (kg/m^3)	Heat capacity (J/kg K)	Thermal conductivity (W/m K)
Copper	37,136	7924	385	398
Al_2O_3 nanoparticle layer	11,819	3820	880	12

Table 4
Average surface characteristics of all specimens.

Flow velocity (m/s)		Roughness (nm)	Static contact angle for water (°)	CHF Enhancement ratio (%)
	Bare copper	800 (±20)	75 (±3)	–
v = 0	Water-boiled copper	900 (±14)	68 (±1.3)	–
	Nanofluid-boiled copper	1840 (±364)	12 (±1.2)	51
v = 1	Water-boiled copper	812 (±12)	65 (±0.6)	–
	Nanofluid-boiled copper	1574 (±273)	46.5	24
v = 2	Water-boiled copper	778 (±6)	66 (±0.8)	–
	Nanofluid-boiled copper	1510 (±170)	42.1	25
v = 3	Water-boiled copper	823 (±10)	65 (±3.2)	–
	Nanofluid-boiled copper	1358 (±505)	34.1 (±9.3)	42
v = 4	Water-boiled copper	796 (±18)	62 (±1.8)	–
	Nanofluid-boiled copper	1114 (±297)	18.3 (±0.4)	40

CHF enhancement ratio (%) = $CHF_{nanofluid}/CHF_{purewater}$ at a given flow velocity.

Table 3 summarizes the thermo-physical properties of the heater materials of interest in this study. Thermal effusivity is a representative parameter for transient heat conduction within the heater, and the higher effusivity of the heater material can cause the hot/dry spot to be dissipated more effectively (Arik and Bar, 2003). However, the alumina nanoparticles layer has smaller effusivity than copper, i.e., 37,136 J/(m K s$^{1/2}$) for copper vs. 11,819 J/(m K s$^{1/2}$) for alumina.

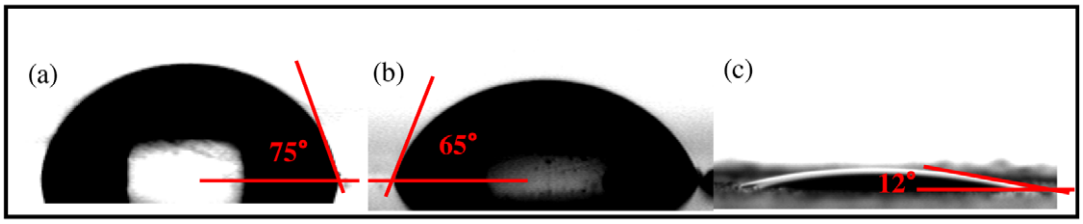

Fig. 9. Contact angle of a water droplet on the heating surfaces: (a) the as-received surface; (b) the water-boiled surface at 3 m/s; and (c) the nanofluid-CHF-boiled surface at 0 m/s.

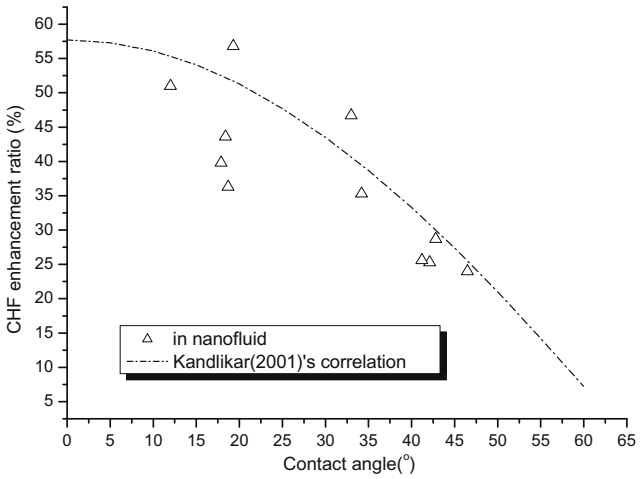

Fig. 10. Relationship between the flow boiling CHF enhancements and the contact angle of a water droplet on the heater surfaces in all fluid velocity.

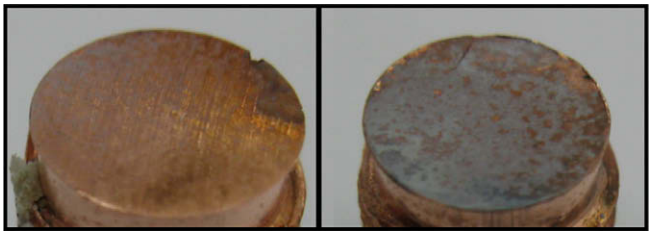

Fig. 11. Different deposition of nanoparticles at 3 m/s, after CHF test; CHF: (left): 3638 kW/m^2 (right): 4435 kW/m^2.

Next, the roughness of the nanoparticles-fouled surface is significantly larger than that of the clean surface, because of the peak-and-valley structures of the nanoparticles deposition. Table 4 shows the surface roughness values of various heating surfaces on which the flow boiling CHF experiments of nanofluid were performed. It is found that the roughness change on the nanofluid-boiled surfaces does not correlate the CHF enhancement ratio.

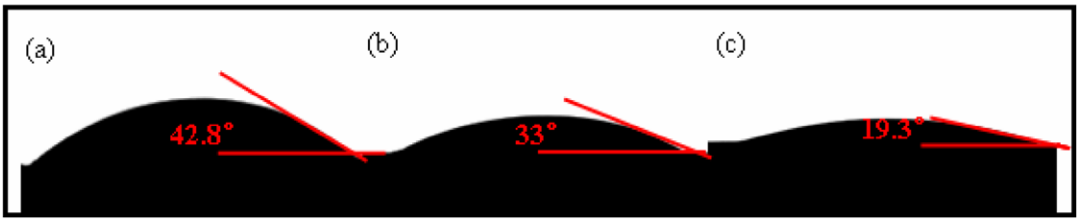

Fig. 12. Contact angles of water droplets on the nanoparticle-deposited surfaces at 3 m/s CHF: (a) 3638 kW/m^2; (b) 4147 kW/m^2; (c) 4435 kW/m^2.

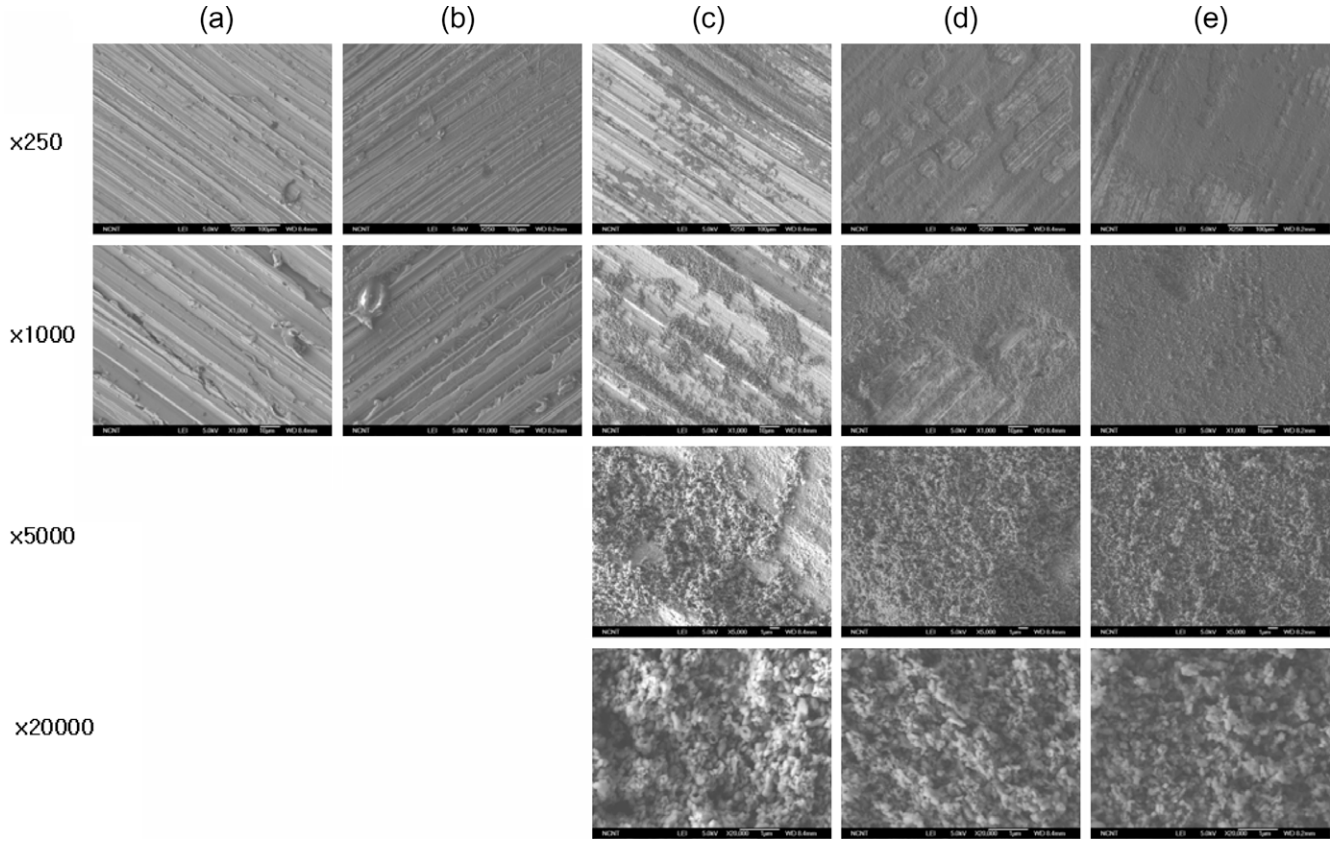

Fig. 13. SEM images of the heater surfaces: (a) as-received; (b) water-boiled and q''_{CHF} = 1486 kW/m^2; (c) nanofluid boiled at 3 m/s and q''_{CHF} = 3827 kW/m^2; (d) nanofluid boiled at 3 m/s and q''_{CHF} = 4147 kW/m^2; and (e) nanofluid boiled at 4 m/s and q''_{CHF} = 4920 kW/m^2.

According to Hahne and Grigull (1977), the surface roughness affects the vapor bubble growth due to the distribution and activation of nucleation sites, but the effects of changing density of active nucleation sites are relatively weak near the peak heat flux. This was mainly confirmed by the fact that the roughness shows no effect on the CHF values (Tong, 1968). In fact, Kim et al. (2006b, 2009a,b) noted that the roughness increase due to nanoparticles deposition does not correlate with the CHF values measured on the nanoparticles-fouled surfaces. The surface wettability effect on the nanoparticles-fouled surface shall be discussed in the next section.

3.3. CHF enhancement in nanofluid and wettability

Fig. 9 compares the contact angle of a water droplet on the as-received, water-boiled, and alumina nanoparticles-fouled surfaces with no flow condition. The contact angle on the fouled surface, ~12°, is significantly smaller than on the water-boiled surface, ~65°, indicating that the fouled surface is more wettable. The strong influence of surface wettability on the CHF enhancement is well-known. Kandlikar (2001) proposed a theoretical model for pool boiling CHF incorporating contact angle,

$$q''_{CHF} = h_{fg}\rho_g^{1/2}\left(\frac{1+\cos\beta}{16}\right)\left[\frac{2}{\pi}+\frac{\pi}{4}(1+\cos\beta)\cos\phi\right]^{1/2}[\sigma g(\rho_l-\rho_g)]^{1/4} \quad (7)$$

where β is the contact angle of substrate, ϕ the originated angle, h_{fg} the latent heat (J/kg), and g the gravity (m/s^2). If contact angle changes from 65° (for a water-boiled surface) to 12° (for the nanoparticles-fouled surface), Eq. (7) predicts a CHF enhancement of about 55%, which is close to the results observed in our experiments. Thus, the improved wetting of fluid on a surface due to the nanoparticles deposition is likely an interfacial parameter responsible for the CHF enhancement under pool boiling in nanofluids.

Fig. 10 shows the relationship between the flow boiling CHF enhancements in nanofluids, obtained from the ratio of the nanofluid value to the pure water value at each flow velocity, and the static contact angles of a water droplet on the used heater surfaces. Also, a prediction of Kandlikar's (2001) pool boiling CHF correlation for the CHF change due to the contact angle reduction below 65°, which was measured for the water-boiled surface, was also plotted. Interestingly, the flow boiling CHF enhancement data (normalized CHF enhancement at a given flow velocity) in the present study appear to be well correlated with the contact angles on the nanofluid-boiled surfaces regardless of the flow velocities. Furthermore, the experimental results show the same trend as the prediction of Kandlikar's (2001) pool boiling CHF correlation for the CHF

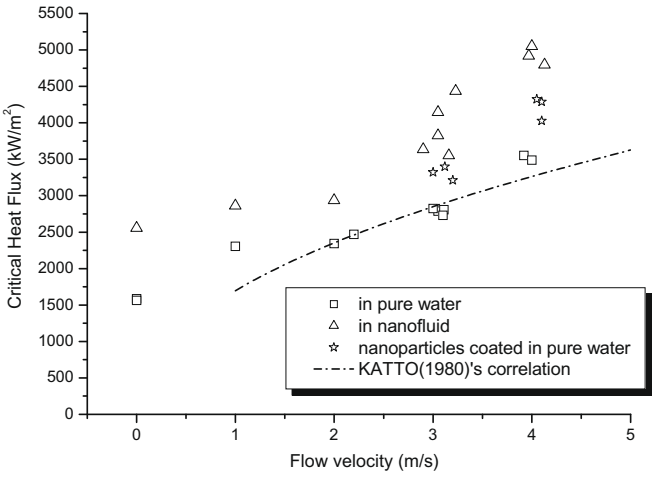

Fig. 14. Comparisons of CHF values for pure water and nanofluid on the clean surface, and pure water on a nanoparticles-coated surface.

enhancement by the contact angle reduction of a water droplet on the heater surface below 65°. The results show that the flow boiling CHF enhancement in nanofluid is strongly related to surface wettability, similar to the pool boiling CHF enhancement. Though, the flow velocity is same, some nanofluid CHF data show the major data scattering, e.g., at 3 m/s the CHF enhancements of three runs were 29%, 47%, and 57%. These scatters were also found in Fig. 7, where previously was mentioned. However, it was found that even at the same velocity condition, the amount of nanoparticles deposition could be considerably different, as shown in Fig. 11, thus resulting in the different contact angles (see Fig. 12). The difference in contact angles properly explains the scatter in the CHF enhancement data at the same flow velocity. Therefore, all our experimental results indicate that the key parameter to explain the nanofluid flow boiling CHF enhancement is the improved surface wettability due to the nanoparticles deposition.

3.4. Ad-hoc tests to confirm the nanoparticles deposition effect

Some additional tests for flow boiling CHF of pure water on nanoparticles-fouled surfaces were conducted to have the consistence of effect of nanoparticles deposition on the CHF enhancement. We purposed the reappearance of CHF enhancement in pure water to support the effect of nanoparticles deposition on heating surface under flow boiling. At a given flow velocity in

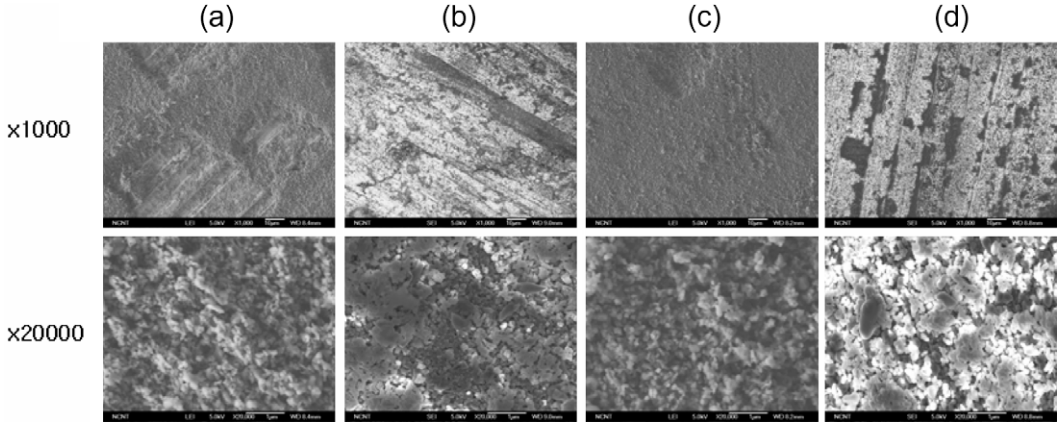

Fig. 15. SEM images of nanoparticles coated specimens: (a) nanoparticles-coated surface in nanofluid at 3 m/s; (b) after pure water boiling test of nanoparticles-coated surface in nanofluid at 3 m/s; (c) nanoparticles-coated surface in nanofluid at 4 m/s; and (d) after pure water boiling test of nanoparticles-coated surface in nanofluid at 4 m/s.

Table 5
Average surface characteristics of coated surface.

	Flow velocity (m/s)	Roughness (nm)	Static contact angle for water (°)	CHF Enhancement ratio (%)
$v = 3$	Nanofluid-boiled	1358 (±505)	34.1 (±9.3)	42
	Nanoparticles-coated	1740 (±297)	10 (±2.9)	–
	Water-boiled nanoparticles coated	756 (±191)	45.2 (±3.3)	17
$v = 4$	Nanofluid-boiled	1114 (±297)	18.3 (±0.4)	40
	Nanoparticles-coated	Not measured	9.2 (±2.1)	–
	Water-boiled nanoparticles coated	848 (±156)	28.5 (±6.3)	20

CHF enhancement ratio (%) = $CHF_{nanofluid}/CHF_{purewater}$ at a given flow velocity.

nanofluid, the CHF would increase as previously mentioned. However, one question was remained whether the flow momentum could detach the nanoparticles on heating surface, or not. Two sets of nanoparticles-coated surfaces for flow boiling tests of pure water at 3 m/s and 4 m/s were prepared by the exactly same procedures as the flow boiling experiment of nanofluids at the same flow velocities, respectively. But to prevent the heater surface being altered and/or damaged during CHF phenomena, heat flux increase during the coating process was limited up to 90% of the average CHF of nanofluid at a given velocity. Then, the flow boiling experiments in pure water was conducted at the same flow velocity.

As shown in Fig. 14, CHF of pure water on the nanoparticles coated specimens was higher than the value of pure water on a bare surface but lower than that of the nanofluid, though we expected the same CHF enhancement in pure water with the nanoparticles-coated surface vs. the enhancement in nanofluid. It was found from a comparison of SEM images of the coated surfaces before and after the water boiling tests that the considerable amount of nanoparticles were detached from the coated surface while heat flux gradually increased for flow boiling of pure water (see Fig. 15). Consequently, surface roughness of the coated surfaces decreased from 1740 nm to 756 nm and static contact angle increased from ~10° to 45°, as given in Table 5. As a result, the CHF enhancement of pure water on the nanoparticles-coated surfaces became smaller than the CHF value in nanofluid. On the conclusion, the detachment of nanoparticles on heating surface could influence the change of surface characteristics, finally influenced the lower CHF enhancement than case in nanofluid.

4. Conclusion

Flow boiling CHF enhancement phenomena in water-based 0.01 vol.% alumina nanofluids was investigated as changing flow velocity from 0 m/s to 4 m/s. The findings in the study are as follows:

- Flow boiling CHF increased in nanofluids relative to in pure water, and the enhancement ratio increased as increasing flow velocity, e.g. 24% at 1 m/s and 40% at 4 m/s. Since the CHF enhancement by convective flow was higher in nanofluid than in pure water, it was explained the surface wettability effect which was induced the nanoparticles deposition by the boiling.
- Nano-micro scale structures were formed during nanofluid flow boiling and changed surface morphology significantly. However, only the roughness change was not enough to interpret the CHF enhancements in nanofluids.
- Changes in surface wettability due to the nanoparticles deposition found to be a key parameter to account for CHF enhancements in nanofluid. The experimental results revealed that flow velocity and surface wettability independently affected on CHF enhancement phenomena in nanofluids. Normalized CHF enhancement data and static contact angle data have a good agreement with pool boiling CHF model, which have an effect of wettability.
- Ad-hoc tests were performed to verify the effect of nanoparticles deposition on the heating surface. The CHF of nanoparticles coated specimen at a given flow velocity in pure water increased more than a bare specimen in pure water, however increased lower than in nanofluid. It was explained by the nanoparticles detachment, which was investigated by SEM image and roughness and static contact angle data. Finally, nanoparticles detachment under flow boiling could influence lower CHF than in nanofluid.

Acknowledgments

This research was supported by KAERI (KOREA ATOMIC ENERGY RESEARCH INSTITUTE), the support being a generous gift from Dr. DaeHyun Hwang and Dr. ChiWoong Choi.

References

Ahn, H.S., Kim, S., Jo, H.J., Kim, D.E., Kang, S.H., Kim, M.H., 2008a. An experimental study of forced convective flow boiling CHF in nanofluid, NTHAS6, Okinawa, Japan, November 24–27.
Ahn, H.S., Kim, S., Jo, H.J., Kim, M.H., 2008b. Pool boiling CHF enhancement in nanofluids using a flat plate heater, Transactions of the Korean Nuclear Society Spring Meeting, Gyeongju, Korea, May 29–30.
Arik, M., Bar, A.C., 2003. Effusivity-based correlation of surface property effects in pool boiling CHF of dielectric liquids. Int. J. Heat Mass Transfer 46, 3755–3764.
Bang, I.C., Chang, S.H., 2005. Boiling heat transfer performance and phenomena of Al_2O_3–water nano-fluids from a plain surface in a pool. Int. J. Heat Mass Transfer 48, 2407–2419.
Choi, S.U., 1995. Enhancing thermal conductivity of fluids with nanoparticles. In: Siginer, D.A., Wang, H.P. (Eds.), Developments and Applications of Non Newtonian flows, FED-Vol. 231/MD-Vol. 66. ASME, New York, pp. 99–105.
Chowdhury, S.K.R., Winterton, R.H.S., 1985. Surface effects in pool boiling. Int. J. Heat Mass Transfer 28, 1881–1889.
Coleman, H.W., Steele, W.G., 1999. Experimentation and uncertainty analysis for engineers, second ed. John Wiley & Sons, Inc..
Coursey, J.S., Kim, J., 2008. Nanofluid boiling: the effect of surface wettability. Int. J. Heat Fluid Flow 29, 1577–1585.
Golubovic, M., Hettiarachchi, M.H.D., Worek, W.M., 2008. Nanofluids and critical heat flux. In: Paper No. MNHT2008-52204, Proceedings of 1st ASME Micro/Nanoscale Heat Transfer International Conference, Tainan, Taiwan.
Hahne, E., Grigull, U., 1977. Heat Transfer in Boiling. Hemisphere, New York.
Kandlikar, S.G., 2001. A theoretical model to predict pool boiling chf incorporating effects of contact angle and orientation. J. Heat Transfer 123, 1071–1080.
Katto, Y., Kurata, C., 1980. Critical heat flux of saturated convective boiling on uniformly heated plates in a parallel flow. Int. J. Multiphase Flow 6, 575–582.
Kim, H., 2007. Experimental investigations of pool boiling CHF enhancement in nanofluids, Ph.D. thesis, POSTECH, Pohang, Republic of Korea.
Kim, H.D., Kim, M.H., 2007. Effect of nanoparticle deposition on capillary wicking that influences the critical heat flux in nanofluids. Appl. Phys. Lett. 91, 014104.
Kim, H., Kim, J., Kim, M.H., 2006a. Effect of nanoparticles on CHF enhancement in pool boiling of nano-fluids. Int. J. Heat Mass Transfer 42, 2003–2013.
Kim, H., Kim, J., Kim, M.H., 2006b. Experimental study on the characteristics and mechanism of pool boiling CHF enhancement using nano-fluids. In: ECI International Conference on Boiling Heat Transfer, Spoleto, May 7–12.
Kim, H.D., Kim, J., Kim, M.H., 2007a. Experimental studies on CHF characteristics of nano-fluids at pool boiling. Int. J. Multiphase Flow 33, 691–706.
Kim, S.J., Bang, I.C., Buongiorno, J., Hu, L.W., 2007b. Surface wettability change during pool boiling of nanofluids and its effect on critical heat flux. Int. J. Heat Mass Transfer 50, 4105–4116.
Kim, S.J., McKrell, T., Buongiorno, J., Hu, L.W., 2008. Experimental study of flow critical heat flux in low concentration water-based nanofluids. In: Proceedings of MNHT2008.
Kim, H., Dewitt, G., Mckrell, T., Buongiorno, J., Hu, L.W., 2009a. On the quenching of steel and zircaloy spheres in water-based nanofluids with alumina, silica and diamond nanoparticles. Int. J. Multiphase Flow 35, 427–438.

Kim, S.J., McKrell, T., Buongiorno, J., Hu, L.W., 2009b. Experimental study of flow critical heat flux in alumina–water, zinc-oxide–water, and diamond–water nanofluids. J. Heat Transfer 131, 043204-1.

Kim, H., Ahn, H.S., Kim, M.H., 2010. On the mechanism of pool boiling critical heat flux enhancement in nanofluids. J. Heat Transfer.

Kutateladze, S.S., 1950. A hydrodynamic model of the critical heat transfer in boiling liquids with free convection. Zhurn, Tekh. Fiz. 20, 1389–1392.

Liter, S.G., Kaviany, M., 2001. Pool-boiling CHF enhancement by modulated porous-layer coating: theory and experiment. Int. J Heat Mass Transfer 44, 4287–4311.

Liu, Z., Liao, L., 2008. Sorption and agglutination phenomenon of nanofluids on a plane heating surface during pool boiling. Int. J. Heat Mass Transfer 51, 2593–2601.

Milanova, D., Kumar, R., 2005. Role of ions in pool boiling heat transfer of pure and silica nanofluids. Appl. Phys. Lett. 87, 233107.

Moreno Jr., G., Oldenburg, S.J., You, S.M., Kim, J.H., 2005. Pool boiling heat transfer of alumina–water, zinc oxide–water and alumina–water + ethylene glycol nanofluids. In: Proceedings of HT2005 2005 ASME Summer Heat Transfer Conference, July 17–22, 2005, San Francisco, California, USA.

Murshed, S.M.S., Leong, K.C., Yang, C., 2005. Enhanced thermal conductivity of TiO_2–water based nanofluids. Int. J. Therm. Sci. 44, 367–373.

Park, H.S., Shiferaw, D., Sehgal, B.R., Kim, D.K., Muhammed, M., 2004. Film boiling heat transfer on a high temperature sphere in nanofluid. In: Proceedings of ASME HT/FED, vol. 4, pp. 469–476.

Santillan, M.J., Membrives, F., Quaranta, N., Boccaccini, A.R., 2008. Characterization of TiO_2 nanoparticle suspensions for electrophoretic deposition. J. Nanoparticle Res. 10, 787–793.

Tong, L.S., 1968. Boiling Heat Transfer and Two Phase Flow. Wiley, New York.

Vassallo, P., Kumar, R., D'Amico, S., 2004. Pool boiling heat transfer experiments in silica–water nano-fluids. Int. J. Heat Mass Transfer 47, 407–411.

Wen, D., Ding, Y., 2005. Experimental investigation into the pool boiling heat transfer of aqueous based c-alumina nanofluids. J. Nanoparticle Res. 7, 265–274.

You, S.M., Kim, J.H., Kim, K.H., 2003. Effect of nanoparticles on critical heat flux of water in pool boiling heat transfer. Appl. Phys. Lett. 83, 3374–3376.

Zuber, N., 1959. Hydrodynamic aspects of boiling heat transfer. Ph.D. thesis, University of California, Los Angeles, USA.